![THE UNIVERSITY of EDINBURGH]

Edinburgh Research Explorer

Depletion of Drad21/Scc1 in Drosophila cells leads to instability of the and disruption of mitotic cohesin complex progression

OPEN ACCESS

Depletion of Drad21/Scc1 in *Drosophila* Cells Leads to Instability of the Cohesin Complex and Disruption of Mitotic Progression

Sharron Vass,[1] Sue Cotterill,[2] Ana M. Valdeolmillos,[3]
José L. Barbero,[3] Enmoore Lin,[4]
William D. Warren,[4,5] and Margarete M.S. Heck[1,*]
[1] Wellcome Trust Centre for Cell Biology
Institute of Cell and Molecular Biology
University of Edinburgh
Michael Swann Building
King's Buildings
Mayfield Road
Edinburgh EH9 3JR
[2] Department of Biochemistry and Immunology
Street Georges Hospital Medical School
Cranmer Terrace
London SW17 ORE
United Kingdom
[3] Department of Immunology and Oncology
Centro Nacional de Biotecnología
UAM campus de Cantoblanco
Madrid E-28049
Spain
[4] Trescowthick Research Laboratories
Peter MacCallum Cancer Institute
Street Andrews Place
East Melbourne, Victoria 3002
Australia

Summary

Background: The coordination of cell cycle events is necessary to ensure the proper duplication and dissemination of the genome. In this study, we examine the consequences of depleting Drad21 and SA, two non-SMC subunits of the cohesin complex, by dsRNA-mediated interference in *Drosophila* cultured cells.
Results: We have shown that a bona fide cohesin complex exists in *Drosophila* embryos. Strikingly, the Drad21/Scc1 and SA/Scc3 non-SMC subunits associate more intimately with one another than they do with the SMCs. We have observed defects in mitotic progression in cells from which Drad21 has been depleted: cells delay in prometaphase with normally condensed, but prematurely separated, sister chromatids and with abnormal spindle morphology. Much milder defects are observed when SA is depleted from cells. The dynamics of the chromosome passenger protein, INCENP, are affected after Drad21 depletion. We have also made the surprising observation that SA is unstable in the absence of Drad21; however, we have shown that the converse is not true. Interference with Drad21 in living *Drosophila* embryos also has deleterious effects on mitotic progression.
Conclusions: We conclude that Drad21, as a member of a cohesin complex, is required in *Drosophila* cultured cells and embryos for proper mitotic progression. The

protein is required in cultured cells for chromosome cohesion, spindle morphology, dynamics of a chromosome passenger protein, and stability of the cohesin complex, but apparently not for normal chromosome condensation. The observation of SA instability in the absence of Drad21 implies that the expression of cohesin subunits and assembly of the cohesin complex will be tightly regulated.

Introduction

The faithful transmission of genetic material during the cell cycle requires exquisite orchestration. During interphase, the genome is accurately replicated to form two identical sister chromatids, which are held in close proximity to permit DNA repair and recombination, and to ensure accurate segregation during the ensuing mitosis. The sister chromatids are then coordinately condensed and resolved in order to permit segregation without tangling or damage to the genome. Once surveillance checkpoints monitoring genome integrity and kinetochore attachment to microtubules are satisfied, cohesion is dissolved, and the chromosomes are segregated to two daughter cells.

Diverse approaches have been utilized to identify and characterize the components necessary for mitosis. The identification of the SMC (Structural Maintenance of Chromosomes) genes in yeast and the purification from *Xenopus* extracts of cohesin and condensin complexes in which the SMC proteins are found associated with non-SMC subunits has profoundly influenced our thinking of chromosome dynamics (reviewed in [1–5]). The genes for cohesin and condensin components have been identified in all eukaryotes examined; biochemical purification of cohesin complexes was achieved in *Xenopus* and human cells [6–8], and that of condensin complexes was achieved in *S. pombe* and *Xenopus* [9, 10]. The genetic analysis of cohesin and condensin subunits is ongoing in yeast, *Drosophila*, and chicken cells. Thus, there is still much information to be gleaned from diverse systems, particularly those amenable to combined genetic and high-resolution cytological analysis.

While it is tempting to generalize from one system about the structure, function, and regulation of cohesin and condensin complex activity in other organisms, one of the most intriguing findings about the cohesin complex has resulted from the comparison of sister chromatid dissolution in single- and multicellular eukaryotes. In *S. cerevisiae*, Scc1p becomes associated with chromatin upon replication and can be detected all along the chromosome arms until the metaphase-to-anaphase transition, when Scc1p is cleaved by "separase" [11, 12]. However, in *Drosophila*, *Xenopus*, and human cells, the majority of Scc1 dissociates from chromosome arms during prophase after Polo kinase phosphorylation [13], with a small centromeric pool remaining until chromosomes are disjoined at the onset of anaphase [8, 13, 14].

We have been characterizing cohesin and condensin

*Correspondence: margarete.heck@ed.ac.uk
[5] Present address: Comparative Genomics Center, James Cook University, Townsville, Queensland 4811, Australia.

components in *Drosophila* with the aim to understand their localization and function in a system amenable to cytological and genetic analysis [15, 16]. To date, there are no known *Drosophila* mutant alleles of *Scc1* (known as *Drad21* [16]), precluding a conventional genetic analysis of this gene. However, dsRNA-mediated interference (RNAi) in *Drosophila* cultured cells has been used to successfully create a genetic null or strong depletion phenotype of many genes [17, 18].

We demonstrate here that Drad21 is indeed part of a bona fide complex in *Drosophila* embryos. As in *Xenopus* and human cells, this complex contains SMC1, SMC3, Drad21, and SA (also known as Scc3) [6]. Strikingly, Drad21 and SA appear to be more tightly associated to each other than they are to the SMCs. In this study, we have characterized the phenotype of *Drosophila* cultured cells depleted of Drad21 and SA. We clearly show that cells depleted of Drad21 are delayed in prometaphase and have prematurely separated (although normally condensed) sister chromatids; this phenotype is not observed when SA is depleted. The prometaphase delay results in altered dynamics of the chromosomal passenger INCENP protein [19]. Additionally, we show that the stability of SA is dependent on the presence of Drad21, but that the converse is not true. These findings extend significantly our understanding of the dynamics of cohesin subunits in multicellular eukaryotes and raise new questions about the coordination of assembly and activity of the cohesin complex.

Results

Specific Depletion of Drad21 by dsRNA-Mediated Interference in *Drosophila* Cultured Cells

The *Drad21* gene is comprised of 8 exons giving rise to a 2.3-kb cDNA, encoding a predicted protein of 715 amino acids [16]. Although the *Drad21* locus has been entirely sequenced, its exact location in the genome remains unclear. DNA in situ hybridization on salivary gland polytene chromosomes showed hybridization to the chromocenter, suggesting that the *Drad21* gene is embedded within heterochromatin.

Because of the lack of mutations in the *Drad21* gene, we used dsRNAi in S2 cultured cells [17, 18] to analyze the consequence on mitotic events of Drad21 loss. Cells were incubated with a ∼650-bp dsRNA that incorporated the ATG, while a similar length dsRNA from a cloned human intron served as control [20]. We analyzed cell extracts by immunoblotting at various time points after treatment. A decrease in the level of Drad21 protein was apparent as early as 24 hr after treatment; this depletion continued until 96 hr after treatment, when the protein was barely detectable (Figure 1A). As we could detect Drad21 in as few as 10^4 cells and since 5×10^5 cells were loaded, we concluded that at least 98% of the protein was depleted by 96 hr after treatment. In contrast, there was no depletion of Drad21 in control cells (Figure 1A). Cells examined by immunofluorescence confirmed that the number of Drad21-containing cells decreased dramatically after treatment with Drad21 dsRNA (data not shown).

Loss of Drad21 Destabilizes the SA Subunit of Cohesin

Although the genes for all of the *Drosophila* cohesin components have been identified [1, 16, 21, 22], we demonstrate here for the first time that a cohesin complex exists in *Drosophila*. Drad21 antibody on beads was used to immunoprecipitate proteins from 0- to 5-hr whole embryo extracts. Following washes, bound proteins were eluted with 2% SDS in PBS. The eluate was electrophoresed, and two prominent bands of ∼140–150 kDa were excised and identified by mass spectrometry as the *Drosophila* orthologs of SMC1 and SMC3 (Figure 1B). These two proteins were precipitated in roughly equivalent amounts, consistent with current models of cohesin and condensin complexes in which two different SMCs associate in a 1:1 heterodimer [23, 24]. The anticipated non-SMC subunits were, however, *not* eluted from the Drad21 beads. Immunoblotting for Drad21 and SA proteins indicated that these two proteins were only solubilized after eluting the beads with hot SDS-PAGE sample buffer (Figure 1C, pellet). This result intriguingly suggested that Drad21 and SA were more tightly associated with one another than they were with the SMC subunits of the cohesin complex.

Given this apparent tight association, we analyzed the fate of SA upon depletion of Drad21 in cultured cells. Curiously, when Drad21 was depleted by dsRNAi, the level of SA dropped with kinetics indistinguishable from those of Drad21 depletion, indicating that the SA protein was unstable in the absence of Drad21 (Figure 1D). Scrutiny of the Drad21 and SA sequences confirmed that there was no sequence similarity that would result in the dsRNAi of SA. In comparison, the level of INCENP protein was unchanged during Drad21 depletion (Figure 1D). We performed the converse experiment and examined the fate of Drad21 after depletion of SA (Figure 1E). SA is also depleted from cells by dsRNAi with similar kinetics (disappearing by 72 hr after treatment). However, in this case, the level of Drad21 was unaffected by the disappearance of SA, i.e., Drad21 stability was *not* dependent on the presence of SA.

Depletion of Drad21 Results in Abnormal Chromosome and Spindle Morphology

Microscopy revealed striking abnormalities in chromosome alignment and spindle morphology in cells treated with Drad21 dsRNA. Chromosomes appeared spread throughout cells without alignment on a metaphase plate, while spindles appeared narrow and lacked astral microtubules (Figure 2B, control cells shown in Figure 2A). Quantitation of the frequency of cells positive for histone H3 phosphorylated on Serine 10 (P∼H3) in control and dsRNAi cells revealed a 3-fold relative increase over time in Drad21 dsRNAi cells (Figure 2C). We observed that the chromosome and spindle defects increased significantly as the level of Drad21 decreased, reaching nearly 100% of P∼H3 cells by 96 hr after treatment (Figure 2D). As the largest increase took place between 48 and 72 hr after treatment, the majority of phenotypic analysis was carried out on cells after 60–68 hr of dsRNAi.
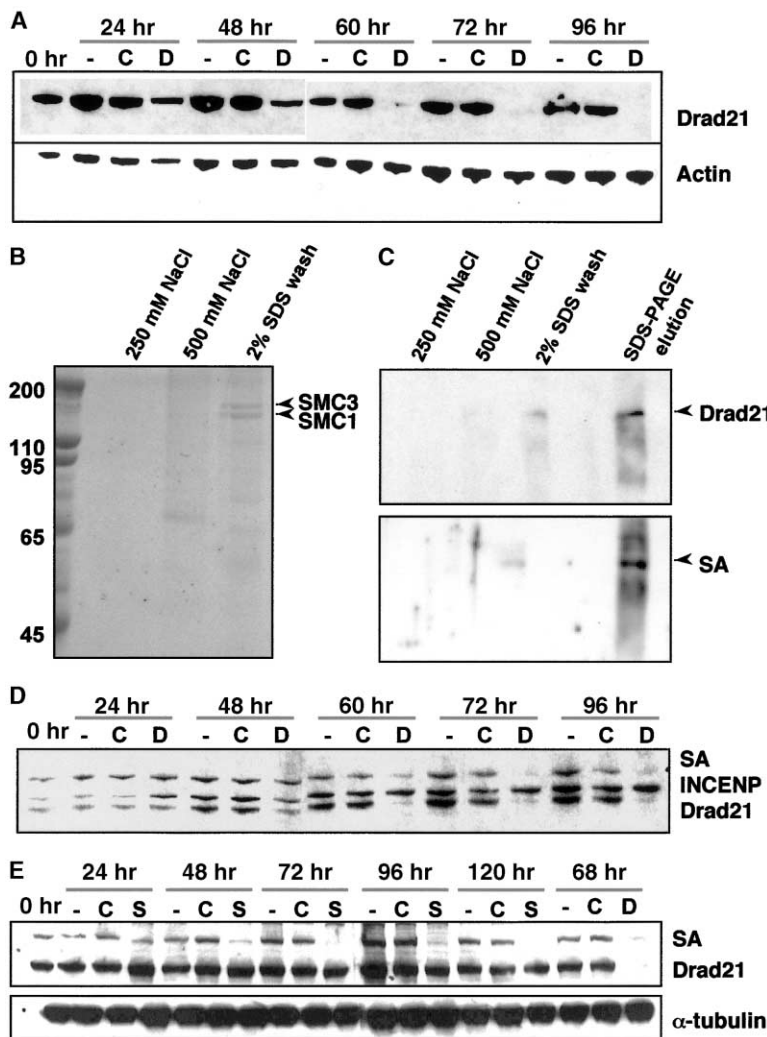
Figure 1. dsRNAi Results in Depletion of the Drad21 Protein and the SA Protein in S2 Cultured Cells

(A) Efficacy of dsRNAi was determined by immunoblotting over time; 5×10^5 cells were loaded per lane. The Drad21 protein level decreased as early as 24 hr after treatment and was undetectable at 96 hr after treatment. Actin was used as a loading control. -, no RNA; C, control RNA; D, Drad21 RNA.

(B) Drad21 exists in a complex with SMC1, SMC3, and SA in *Drosophila* embryos. Immunoprecipitation of Drad21 from 0- to 5-hr embryo extract. NaCl washes and 2% SDS elutions are shown (SMC1 and SMC3 [accession numbers gi/715967 and gi/7447790, respectively] were identified by mass spectrometry).

(C) Immunoblotting for Drad21 shows that the majority of the protein remains associated with the Drad21 antibody-crosslinked beads and is only eluted after boiling in SDS-PAGE sample buffer. Immunoblotting for SA shows that the majority of this protein also remains associated with the Drad21 antibody-crosslinked beads and is only eluted by boiling in sample buffer.

(D) SA is destabilized in cells after Drad21 dsRNA treatment with kinetics similar to those of Drad21 depletion. INCENP serves as a loading control and is not depleted over time. -, no RNA; C, control RNA; D, Drad21 RNA.

(E) SA is depleted from cells after SA dsRNA treatment. Drad21 is stable in the absence of SA. -, no RNA; C, control RNA; S, SA RNA; D, Drad21 RNA. α-tubulin served as a loading control. The final 68 hr time point in this panel is from a Drad21 dsRNAi experiment.

Cells Exhibiting Abnormal Mitotic Morphology Contain Cyclin B

Given that mitotic chromosomes appeared to be distributed along abnormally narrow spindles in cells depleted of Drad21, we wished to determine whether these cells were attempting pre-metaphase chromosome congression or abnormal chromosome segregation. We therefore stained cells for cyclin B and α-tubulin. Cyclin B levels increase during G2, and the protein remains cytoplasmic until nuclear envelope breakdown. During metaphase, the protein is strongly associated with the mitotic spindle and spindle poles (Figure 3A). When cyclin B degradation commences, it does so at the poles, and it progresses along the microtubules until the level of protein becomes indistinguishable from background levels as the cell enters anaphase [25, 26].

The majority of Drad21 dsRNAi cells exhibiting the abnormal mitotic phenotype were cyclin B positive (Figure 3B). As cyclin B was associated with spindles (but the chromosomes had not congressed to a metaphase plate), we concluded that these cells were in prometaphase. While there was very little difference in the frequency of cyclin B-positive cells (Figure 3C, blue bars),

the percentage of cells exhibiting mitotic abnormalities that were cyclin B positive was 87% in the Drad21 dsRNAi cells, compared to <1% in control cells (Figure 3C, green bars).

Cell Cycle Analysis of Drad21-Depleted Cells

Quantitation of the frequency of cells in various stages of mitosis by using P~H3/α-tubulin, and cyclin B/α-tubulin double immunostaining showed that a higher frequency of cells were in prometaphase in the Drad21 dsRNAi cells compared to control cells (Figure 3D). With P~H3/α-tubulin labeling, 33% of untreated and 31% of control dsRNAi mitotic cells were in prometaphase, compared to 70% of Drad21 dsRNAi mitotic cells. This was mimicked by the cyclin B/α-tubulin-labeled cells (41% of untreated and 36% of control dsRNAi mitotic cells were in prometaphase, compared to 64% of Drad21 dsRNAi mitotic cells). However, we also observed cells with abnormal chromosome morphology that lacked cyclin B and appeared to have entered anaphase or telophase, as judged by spindle morphology. Thus, we concluded that the elevated frequency of prometaphase cells was the result of cell cycle delay, but not absolute arrest.
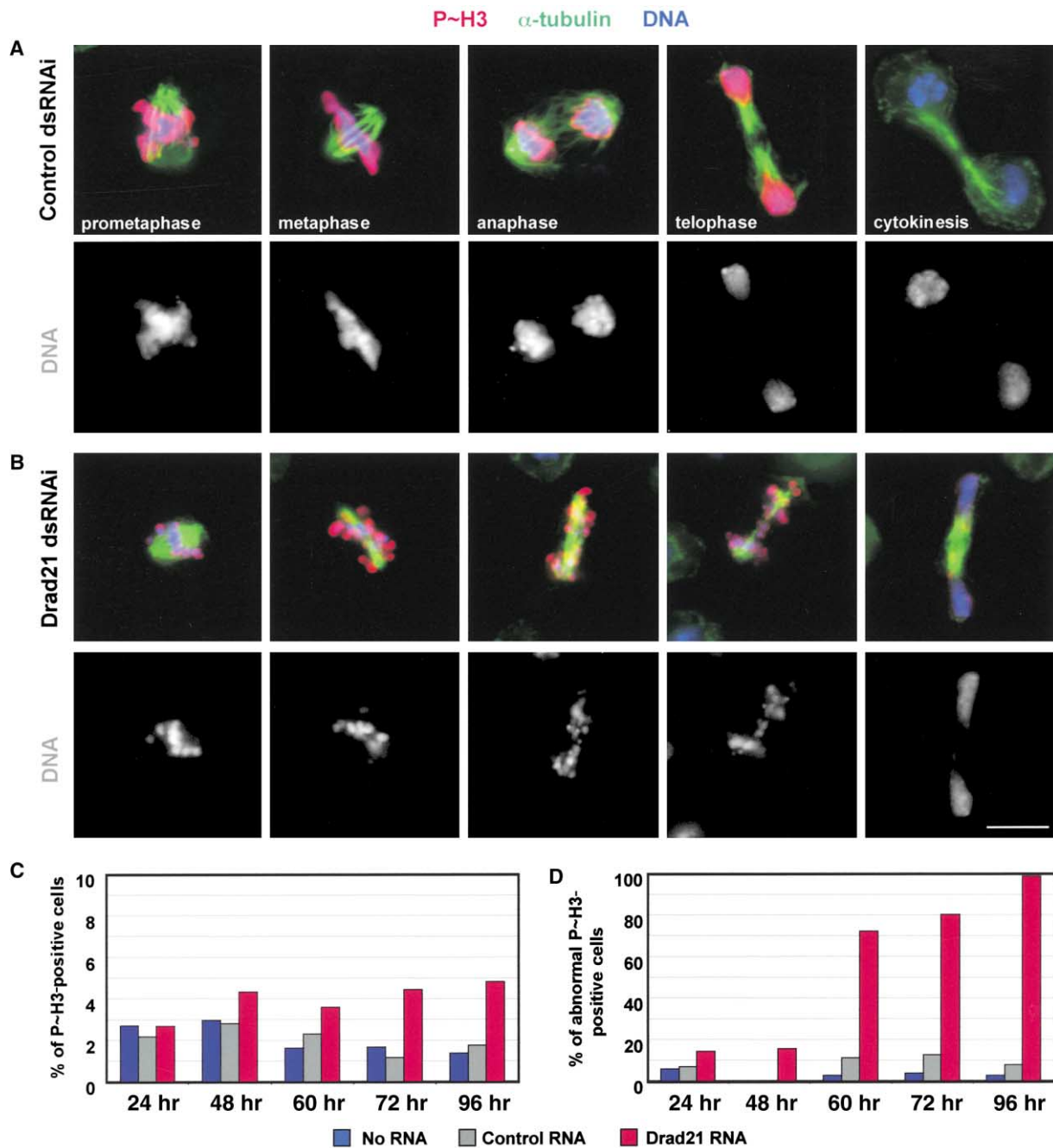
Figure 2. Drad21 Depletion Results in Abnormal Chromosome and Spindle Morphology

(A and B) (A) Control dsRNAi and (B) Drad21 dsRNAi cells were grown on poly-lysine coverslips for 68 hr, then fixed and stained for histone 3 phosphorylated on Serine 10 (P~H3, red), α-tubulin (green), and DNA (DAPI, blue). (A) Various stages of mitosis are indicated in the control panels. (B) Mitotic cells are shown after Drad21 depletion. These cells exhibit defects in chromosome alignment and spindle morphology. The scale bar represents 10 μm.

(C) A graph showing the percentage of cells positive for P~H3 at various time points.

(D) A graph showing the percentage of cells positive for P~H3 that exhibit abnormal mitotic morphology. No RNA is indicated by the blue bars, control RNA is indicated by the gray bars, and Drad21 RNA is indicated by the red bars.

Depletion of SA Results in Apparently Normal Mitotic Progression with Only Rare Defects

A similar analysis to that described above was carried out on cells incubated with SA dsRNA. We were surprised not to detect any significant differences in mitotic progression between SA-depleted and control cells, al- though the protein was barely detectable by 72 hr after treatment (Figure 1E). The frequency of P~H3-positive cells and the frequency of abnormal mitotic cells re- mained the same as control populations (Figure S1). Only at very late time points of 96 and 120 hr did we detect what appeared to be the rare premature resolu-

A Control dsRNAi

B Drad21 dsRNAi

Cyclin B

α-tubulin

DNA

C

No RNA   Control RNA   Drad21 RNA

■ % cells positive for cyclin B
■ % of abnormal cells positive for cyclin B

D

% mitotic cells in specific phase

P~H3   Cyclin B

□ Prophase   ▥ Metaphase   ▨ Telophase
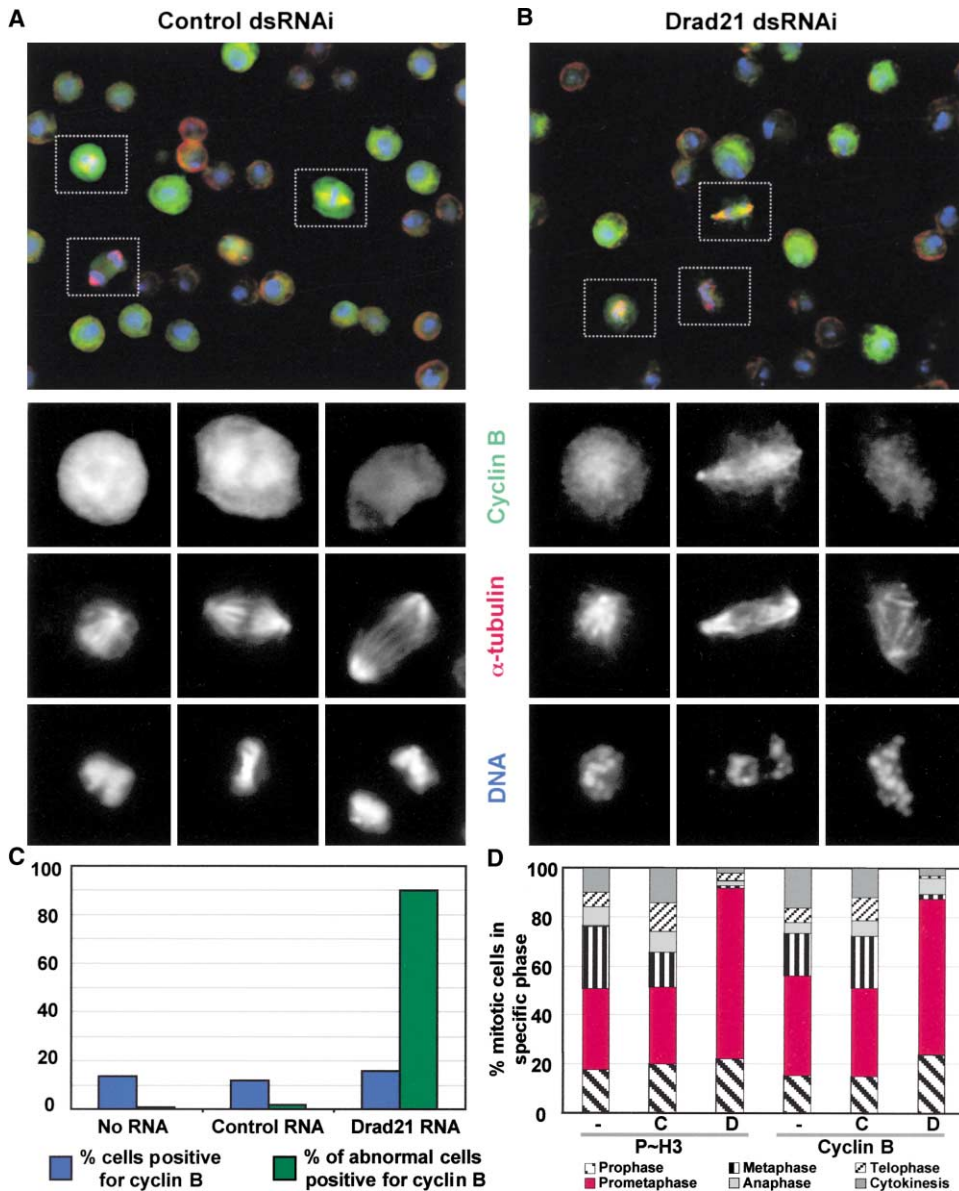▦ Prometaphase   ▨ Anaphase   ▨ Cytokinesis

Figure 3. Cells Exhibiting Abnormal Mitotic Morphology Are Cyclin B Positive

(A and B) (A) Control dsRNAi and (B) Drad21 dsRNAi cells were grown on poly-lysine coverslips for 68 hr, then fixed and immunostained for cyclin B (green), α-tubulin (red), and DNA (DAPI, blue). (A) Normal progression through mitosis with degradation of cyclin B in anaphase is observed. (B) The majority of Drad21-depleted cells exhibiting abnormal mitotic phenotypes stain positively for cyclin B.

(C) A graph depicting the overall percentage of cells positive for cyclin B at 68 hr after treatment (blue bars) and the percentage of cells exhibiting abnormal chromatin morphology that were positive for cyclin B (green bars). Cells exhibiting abnormal mitotic morphology are cyclin B positive.

(D) The distribution of cells among various cell cycle phases, scored for both the P~H3/α-tubulin experiment (Figure 2) and the cyclin B/α-tubulin experiment. The percentage of cells in prometaphase increases with Drad21 dsRNAi (red bars). The number of cells counted for each experiment was: P~H3/α-tubulin: - RNA, 2338; control RNA, 2060; Drad21 RNA, 2315, and cyclin B/α-tubulin: - RNA, 1516; control RNA, 1835; Drad21 RNA, 1486.

tion into distinct chromatids (not chromatid separation) in SA-depleted cells. As this phenotype was not apparent at 72 hr after treatment, present in only 8% of abnormal mitotic cells at 96 hr and in 45% of abnormal mitotic cells at 120 hr, we conclude that it is likely not a direct consequence of SA depletion. Of the two *Drosophila* SA genes, the SA-1 examined here is active during mitosis [22], while the other (SA-2) appears to be required only during meiosis (Sharon Thomas and Bruce McKee, per-

sonal communication), so it is unlikely that SA-2 is substituting for SA-1.

Depletion of Drad21, but Not SA, Results in Premature Sister Chromatid Separation

Although the images of Figures 2B and 3B showed distinct chromosome phenotypes, it was not possible to discern whether cohesion between centromeres was intact in dsRNAi cells. To better examine chromosome

Control dsRNAi | CID | Barren | DNA
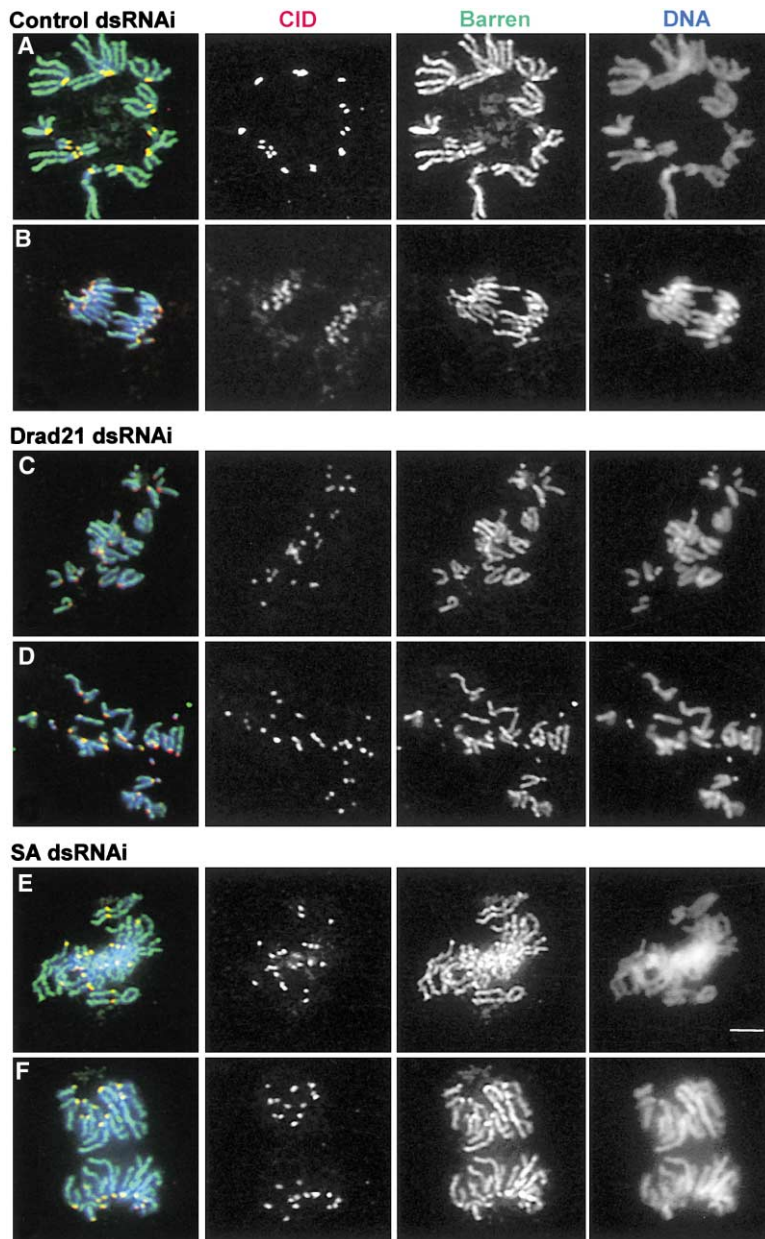
Drad21 dsRNAi

SA dsRNAi

Figure 4. Depletion of Drad21, but Not SA, Results in Premature Sister Chromatid Separation

(A–F) (A and B) Control dsRNAi, (C and D) Drad21 dsRNAi, and (E and F) SA dsRNAi cells were grown in six-well plates, then cytospun onto poly-lysine slides without hypotonic treatment. The cells were fixed and processed for immunofluorescence by using antibodies to CID (red) and Barren (green) and were counterstained with DAPI (blue). (A) A control dsRNAi metaphase cell in which sisters are clearly joined together with two CID spots at the centromere. (B) A control dsRNAi anaphase cell in which sisters have separated and are moving poleward with the centromeres leading. (C and D) Drad21 dsRNAi metaphase cells clearly showing separated sister chromatids, each containing only one CID spot. In contrast to (B), no segregation of chromosomes is evident. (E) An SA dsRNAi metaphase cell clearly showing paired sister chromatids. (F) An SA dsRNAi anaphase cell in which sisters have separated and are moving poleward with the centromeres leading.

morphology in terms of chromatid condensation and pairing after Drad21 and SA depletion, we examined cytospun cells, which facilitated the visualization of individual chromosomes (Figure 4). Importantly, this technique avoids all use of hypotonic solutions that artifactually induce separation of sister chromatids [27]. Control dsRNAi cells showed chromatids tightly paired at the centromere during metaphase (Figure 4A), and then segregating to opposite poles during anaphase (Figure 4B). Drad21-depleted cells clearly showed separated sister chromatids, with each chromatid having one CID spot (CID is the *Drosophila* homolog of CENP-A, a histone H3 isoform found at centromeres [28]) (Figures 4C and 4D). Localization of the non-SMC condensin component, Barren, was normal in the prematurely separated chromatids, and chromosome condensation appeared unaffected at this level of resolution. Chromatids in the

SA-depleted cells did not separate as in the Drad21-depleted cells, although the centromeres appeared to be further apart than in control cells (compare Figure 4E with Figure 4A). Chromosome congression and anaphase separation occurred in the absence of SA (Figure 4F). Analysis of the levels of Barren protein by immunoblotting showed no detectable difference between control or dsRNAi cells (not shown). We conclude that the Drad21 depletion in S2 cells results in premature sister chromatid separation, but that neither Drad21 nor SA depletion has an effect on mitotic chromosome condensation.

Mislocalization of Chromosomal Passenger INCENP Protein in Drad21-Depleted Cells
Although the level of INCENP was unaffected (Figure 1D), the protein showed a striking mislocalization after
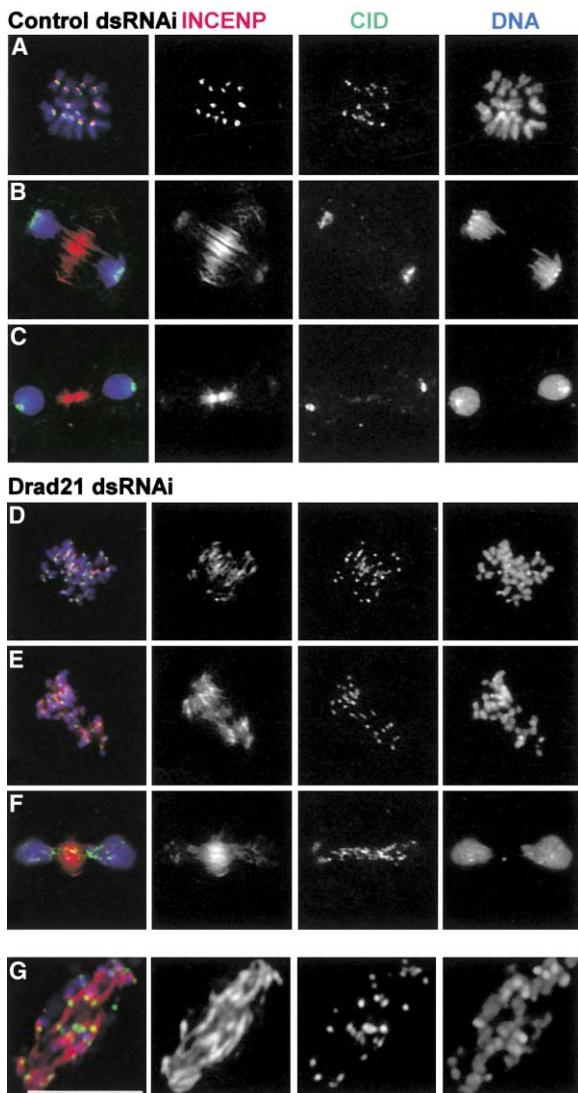
Figure 5. Chromosomal Passenger Protein INCENP Is Mislocalized in Drad21-Depleted Cells

(A–F) (A–C) Control dsRNAi and (D–F) Drad21 dsRNAi cells were cytospun onto poly-lysine slides without hypotonic treatment and were processed for immunofluorescence by using antibodies to INCENP (red) and CID (green); cells were counterstained with DAPI (blue). In control cells, INCENP (A) localizes between CID spots in metaphase, (B) transfers to the spindle in anaphase, and (C) ends up in the midbody. (D and E) In Drad21 dsRNAi cells, INCENP appears more diffuse, (F) though it is still able to migrate to a central region, even when centromeres are abnormally distributed along a mitotic cell.

(G) High-magnification deconvolved images showing INCENP localizing "between" centromeres of separate chromatids in a Drad21 dsRNAi cell. INCENP staining does not appear to colocalize with the bulk of chromatin. The scale bar represents 5 μm.

Drad21 depletion. In control cells, INCENP focused normally (from along the length of chromosomes) to the inner centromere region between CID spots in metaphase and to the spindle midzone in anaphase and telophase (Figures 5A–5C). In Drad21-depleted cells with prematurely separated sisters, INCENP appeared more diffuse and possibly stretched between CID spots (Figures 5D and 5E). However, in later "telophase-like" cells with randomly dispersed (not segregated) centromeres, INCENP adopted the predicted central spindle localization (Figure 5F). High-magnification images of cells similar to those in Figures 5D and 5E showed that INCENP, though not particularly strongly associated with chromatin, appeared to spread between CID spots (whether these were sister or random centromeres was not determined) (Figure 5G).

To determine the mitotic stage of cells exhibiting INCENP mislocalization, we detected INCENP, cyclin B, and α-tubulin in control and Drad21-depleted cells (Figures 6A–6D). In early mitotic cells (high cyclin B), INCENP was dispersed through the spindle and not on the chromosomes as expected (Figure 6C, asterisk). In later mitotic cells (low cyclin B), INCENP was also dispersed throughout the spindle and was not concentrated on the central spindle as predicted (Figure 6D, asterisk). In the few cells undergoing apparent cytokinesis in the Drad21 dsRNAi cultures, INCENP localized normally to the presumptive midbody (Figure 6C, arrowhead). We sorted Drad21-depleted cells with abnormal chromosome morphology and INCENP mislocalization (labeled for α-tubulin and INCENP) into three categories (Figures 6E–6G). The first category contained cells in which INCENP was associated with chromosomes but decorated a more extensive region of the chromosome than the normal discrete centromeric foci (Figure 6E, 64%). The second category contained cells in which INCENP appeared to be transferring to the spindle, although the chromosomes had failed to congress to a metaphase plate (Figure 6F, 10%). The third category contained cells in which most of the INCENP had transferred to the microtubules but failed to form the typical ring at the central spindle normally exhibited by passenger proteins (Figure 6G, 26%). Depletion of the SA protein did not affect the localization of INCENP (data not shown). The lack of centromeric cohesion and congression to a metaphase plate upon Drad21 depletion appears to preclude proper INCENP localization to the centromere and the timely transfer from centromeres to the central spindle (a hallmark of the "chromosomal passenger" proteins). Despite this, late in mitosis, INCENP was still able to localize to microtubules in the central region of the cell.

Loss of Drad21 Function in Embryos by dsRNA Injection also Results in Mitotic Defects

To begin to analyze the effects of Drad21 disruption in the intact organism, we injected dsRNA homologous to the 5′ end of the Drad21 cDNA into syncytial preblastoderm *Drosophila* embryos expressing a histone H2A variant D-GFP fusion [29]. Chromosome condensation and segregation could be readily observed in live embryos by confocal microscopy.

H2AvD-GFP embryos injected with buffer only or with control dsRNA displayed well-distributed and equal-sized nuclei that underwent synchronous mitoses (Figure S2). In contrast, embryos injected with Drad21 dsRNA showed a range of mitotic abnormalities, including delayed chromosome condensation, failure to segregate
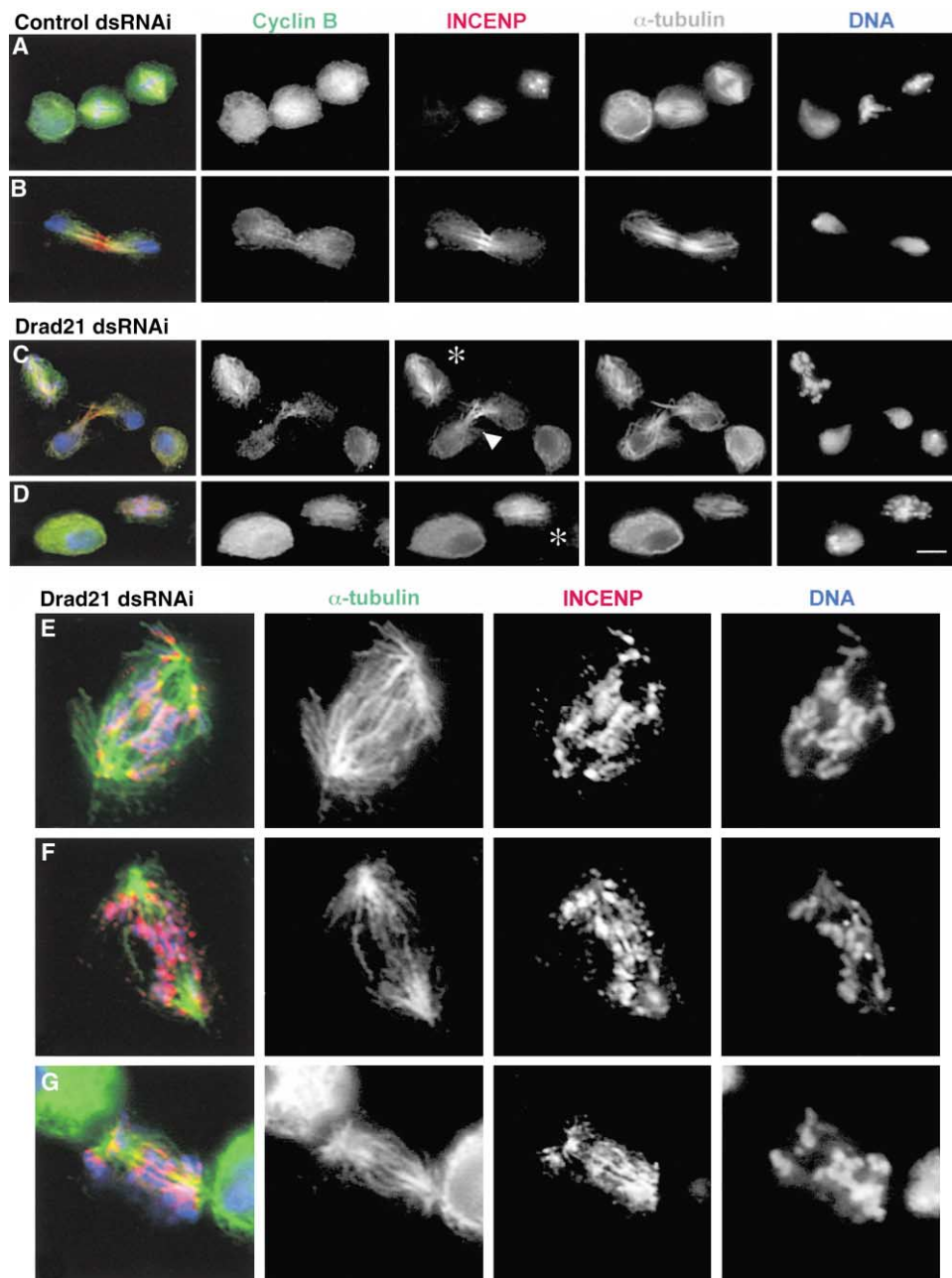
Figure 6. Chromosomal Passenger Protein INCENP Is Mislocalized in Drad21-Depleted Cells

(A–D) (A and B) Control dsRNAi and (C and D) Drad21 dsRNAi cells were grown on poly-lysine coverslips, fixed, processed for immunofluorescence by using antibodies to cyclin B (green), INCENP (red), α-tubulin (white), and counterstained with DAPI (blue). INCENP is localized to centromeres in (A) control metaphase and transfers to the central spindle normally in (B) anaphase. (C) In Drad21-depleted cells, INCENP fails to localize to centromeres when cyclin B is still present (asterisk). The arrowhead highlights a fairly normal cell in cytokinesis with decreased level of cyclin B degradation and highlights INCENP localization to the forming midbody. (D) In another Drad21 dsRNAi cell, INCENP fails to localize to the central spindle when cyclin B is degraded (asterisk). The scale bar represents 5 μm.

(E–G) To further characterize INCENP mislocalization, Drad21-depleted cells were harvested at 68 hr after treatment, cytospun onto poly-lysine slides, then fixed and stained for α-tubulin (green), INCENP (red), and DNA (DAPI, blue). Three categories of mislocalization were observed, and representative cells for each are shown (39 cells were analyzed). (E) A cell showing INCENP associated with chromatin. (F) Some INCENP has translocated to the spindle, but the majority remains associated with chromatin. (G) The majority of INCENP appears to be associated with the microtubules.

chromosomes or unequal chromosome segregation, anaphase bridging, formation of micronuclei, as well as delays or failure of chromosomes to align at metaphase. In the most severely affected embryos, all nuclei ceased dividing and showed chromatin hypercondensation and nuclear aggregation, reminiscent of X-ray-induced DNA damage and DNA damage checkpoint mutant phenotypes [30, 31]. These phenotypes clearly indicate that

Drad21 is required for correct chromosome segregation in early embryos. A detailed characterization of these defects is ongoing.

Discussion

We have demonstrated that Drad21 is in a cohesin complex with SMC1, SMC3, and SA in *Drosophila* embryos. Strikingly, Drad21 and SA are more tightly associated with one another than they are with the SMCs. We have analyzed the consequences of depleting the two non-SMC subunits in *Drosophila* cultured cells, and we have observed that Drad21 depletion results in SA instability; intriguingly, however, the converse is not true. This result suggests that SA must interact with Drad21 in order to be stable (perhaps SA is synthesized only after Drad21 accumulates in the cell). This may help to ensure a 1:1 ratio between these subunits (as observed in cohesin complexes in *S. cerevisiae* [24]). Upon Drad21 depletion, we see dramatic effects on mitotic progression; cells are delayed in prometaphase with prematurely separated sister chromatids and abnormal spindle morphology. In contrast, we observe no premature separation of sister chromatids or significant effects on the cell cycle when SA is depleted, suggesting that the Drad21 phenotype is likely specific to the interference with Drad21 only.

Chromosome condensation in either the Drad21- or the SA-depleted cells appeared normal, as judged by overall size and shape of chromosomes, localization of the Barren non-SMC condensin subunit, and the centromeric domain occupied by the CID centromeric protein. As chromosomes also exhibited normal condensation in Scc1-knockout DT40 cells [32], human cells expressing a dominant-negative N-terminal truncation of Scc1 [33], and after immunodepletion of cohesin from *Xenopus* egg extracts [6], it appears likely that cohesins act independently of condensation machinery in metazoan chromosome structure [6].

The dispersed single chromatids observed in Drad21-depleted *Drosophila* cells were in contrast to the separate, albeit proximal, chromatids after the knockout of Scc1 from DT40 chicken cells [32]. Perhaps for that reason, INCENP appeared along chromosome arms in metaphase Scc1-knockout DT40 cells (INCENP distribution in later mitotic stages was not reported). On the other hand, in early mitotic S2 cells depleted of Drad21, INCENP appeared diffusely localized, possibly because chromatids were no longer close to one another. Later, mitotic cells with aberrant INCENP localization fell into three groups: cells that displayed INCENP staining on single chromatids, cells that showed INCENP transferring onto the spindle even though chromatids had failed to congress to a metaphase plate, and cells in which INCENP associated with microtubules, but was not restricted to the central spindle. Drad21-depleted cells that progressed into the final mitotic stages indicated that INCENP could, however, still localize to the central region of the cell, even though chromosome segregation had not occurred. Our results suggest that the correct localization of INCENP to the centromeric domain and its subsequent translocation to the central spindle at the metaphase-to-anaphase transition is dependent on the presence of cohesion between sister centromeres. However, even in the absence of chromatid cohesion, INCENP was able to achieve microtubule localization, albeit in an abnormal temporal and spatial manner.

It is unlikely that the separate chromatids we observe after Drad21 depletion would form bipolar spindle attachments and align at a metaphase plate. The metaphase checkpoint should be activated, resulting in prometaphase delay (we have observed that centromeres are positive for the BubR1 metaphase checkpoint protein, data not shown). A potential role for sister chromatid cohesion and kinetochore attachment in the metaphase checkpoint has been suggested, with the correct alignment of all sister kinetochores clearly required to establish bipolarity and loss of Mad2 metaphase checkpoint signaling [34, 35]. Why cells are delayed and not arrested by the metaphase checkpoint may be a reflection of compromised checkpoints in *Drosophila* cultured cells (derived from embryos), as these cells are extremely difficult to synchronize in response to numerous cell cycle inhibitors (M.M.S.H. et al., unpublished data).

The mitotic spindles of Drad21-depleted cells appeared abnormally narrow and lacked astral microtubules. Kinetochore microtubules may be unstable in the absence of bipolar attachment and may give rise only to spindle fibers that emanate from poles. Microtubules ending in the cell midzone may be stabilized by components present in the region of overlap, in preference to astral microtubules. A potential role for human cohesin in spindle aster assembly has been suggested, since SMC1 has been localized to the spindle poles during mitosis and interacts with NuMA, a spindle pole-associated protein required for mitotic spindle organization [36]. Recently, the kinase activity of Aurora B was shown to be required for kinetochore-microtubule interactions, and expression of a dominant-negative form resulted in similarly narrow spindles [37]. As Aurora B interacts with INCENP [38, 39], the fate of other chromosome passenger proteins such as Aurora B, TD-60 [40], and survivin [41, 42] should be examined after cohesin interference.

The mitotic failures observed after injection of Drad21 dsRNA into embryos are also consistent with premature loss of sister chromatid cohesion, which ultimately results in segregation defects, aneuploid nuclei, and accumulation of damage to the genome. The most severe phenotypes we observe resemble those of *grapes/chk1* DNA-structure checkpoint mutant embryos, in which damaged nuclei fall into the interior of the embryo [30, 31], and are thus reminiscent of the original DNA-structure checkpoint defects observed in *S. pombe rad21* mutations [43]. The detailed examination of live cells deficient in cohesin or condensin function will contribute greatly to the understanding of mechanisms employed by the cell to ensure genome integrity.

References

1. Cobbe, N., and Heck, M.M. (2000). Review: SMCs in the world of chromosome biology—from prokaryotes to higher eukaryotes. J. Struct. Biol. *129*, 123–143.

2. Cohen-Fix, O. (2001). The making and breaking of sister chromatid cohesion. Cell *106*, 137–140.

3. Hirano, T. (2000). Chromosome cohesion, condensation and separation. Annu. Rev. Biochem. *69*, 115–144.

4. Lee, J.Y., and Orr-Weaver, T.L. (2001). The Molecular basis of sister chromatid cohesion. Annu. Rev. Cell Dev. Biol. *17*, 753–777.

5. Nasmyth, K. (2001). Disseminating the genome: joining, resolving, and separating sister chromatids during mitosis and meiosis. Annu. Rev. Genet. *35*, 673–745.

6. Losada, A., Hirano, M., and Hirano, T. (1998). Identification of *Xenopus* SMC protein complexes required for sister chromatid cohesion. Genes Dev. *12*, 1986–1997.

7. Losada, A., Yokochi, T., Kobayashi, R., and Hirano, T. (2000). Identification and characterization of SA/Scc3p subunits in the *Xenopus* and human cohesin complexes. J. Cell Biol. *150*, 405–416.

8. Sumara, I., Vorlaufer, E., Gieffers, C., Peters, B.H., and Peters, J.M. (2000). Characterization of vertebrate cohesin complexes and their regulation in prophase. J. Cell Biol. *151*, 749–762.

9. Hirano, T., Kobayashi, R., and Hirano, M. (1997). Condensins, chromosome condensation protein complexes containing XCAP- C, XCAP-E and a *Xenopus* homolog of the *Drosophila* Barren protein. Cell *89*, 511–521.

10. Sutani, T., Yuasa, T., Tomonaga, T., Dohmae, N., Takio, K., and Yanagida, M. (1999). Fission yeast condensin complex: essential roles of non-SMC subunits for condensation and Cdc2 phosphorylation of Cut3/SMC4. Genes Dev. *13*, 2271–2283.

11. Blat, Y., and Kleckner, N. (1999). Cohesins bind to preferential sites along yeast chromosome III, with differential regulation along arms versus the centric region. Cell *98*, 249–259.

12. Tanaka, T., Cosma, M.P., Wirth, K., and Nasmyth, K. (1999). Identification of cohesin association sites at centromeres and along chromosome arms. Cell *98*, 847–858.

13. Waizenegger, I.C., Hauf, S., Meinke, A., and Peters, J.M. (2000). Two distinct pathways remove mammalian cohesin from chromosome arms in prophase and from centromeres in anaphase. Cell *103*, 399–410.

14. Warren, W.D., Steffensen, S., Lin, E., Coelho, P., Loupart, M., Cobbe, N., Lee, J.Y., McKay, M.J., Orr-Weaver, T., Heck, M.M., et al. (2000). The *Drosophila* RAD21 cohesin persists at the centromere region in mitosis. Curr. Biol. *10*, 1463–1466.

15. Steffensen, S., Coelho, P.A., Cobbe, N., Vass, S., Costa, M., Hassan, B., Prokopenko, S.N., Bellen, H., Heck, M.M., and Sunkel, C.E. (2001). A role for *Drosophila* SMC4 in the resolution of sister chromatids in mitosis. Curr. Biol. *11*, 295–307.

16. Warren, W.D., Lin, E., Nheu, T.V., Hime, G.R., and McKay, M.J. (2000). Drad21, a *Drosophila* rad21 homologue expressed in S-phase cells. Gene *250*, 77–84.

17. Caplen, N.J., Fleenor, J., Fire, A., and Morgan, R.A. (2000). dsRNA-mediated gene silencing in cultured *Drosophila* cells: a tissue culture model for the analysis of RNA interference. Gene *252*, 95–105.

18. Clemens, J.C., Worby, C.A., Simonson-Leff, N., Muda, M., Maehama, T., Hemmings, B.A., and Dixon, J.E. (2000). Use of double-stranded RNA interference in *Drosophila* cell lines to dissect signal transduction pathways. Proc. Natl. Acad. Sci. USA *97*, 6499–6503.

19. Cooke, C.A., Heck, M.M., and Earnshaw, W.C. (1987). The inner centromere protein (INCENP) antigens: movement from inner centromere to midbody during mitosis. J. Cell Biol. *105*, 2053–2067.

20. Adams, R.R., Maiato, H., Earnshaw, W.C., and Carmena, M. (2001). Essential roles of *Drosophila* inner centromeric protein (INCENP) and Aurora B in histone H3 phosphorylation, metaphase chromosome alignment, kinetochore disjunction, and chromosome segregation. J. Cell Biol. *153*, 865–879.

21. Hong, C.C., and Hashimoto, C. (1996). The maternal nudel protein of *Drosophila* has two distinct roles important for embryogenesis. Genetics *143*, 1653–1661.

22. Valdeolmillos, A., Villares, R., Buesa, J.M., Gonzalez-Crespo, S., Martinez, C., and Barbero, J.L. (1998). Molecular cloning and expression of stromalin protein from *Drosophila melanogaster*: homologous to mammalian stromalin family of nuclear proteins. DNA Cell Biol. *17*, 699–706.

23. Hirano, M., and Hirano, T. (2002). Hinge-mediated dimerization of SMC protein is essential for its dynamic interaction with DNA. EMBO J. *21*, 5733–5744.

24. Haering, C.H., Lowe, J., Hochwagen, A., and Nasmyth, K. (2002). Molecular architecture of SMC proteins and the yeast cohesin complex. Mol. Cell *9*, 773–788.

25. Huang, J., and Raff, J.W. (1999). The disappearance of cyclin B at the end of mitosis is regulated spatially in *Drosophila* cells. EMBO J. *18*, 2184–2195.

26. Whitfield, W.G., Gonzalez, C., Maldonado-Codina, G., and Glover, D.M. (1990). The A- and B-type cyclins of *Drosophila* are accumulated and destroyed in temporally distinct events that define separable phases of the G2-M transition. EMBO J. *9*, 2563–2572.

27. Ohnuki, Y. (1968). Structure of chromosomes. I. Morphological studies of the spiral structure of human somatic chromosomes. Chromosoma *25*, 402–428.

28. Blower, M.D., and Karpen, G.H. (2001). The role of *Drosophila* CID in kinetochore formation, cell-cycle progression and heterochromatin interactions. Nat. Cell Biol. *3*, 730–739.

29. Clarkson, M., and Saint, R. (1999). A His2AvDGFP fusion gene complements a lethal His2AvD mutant allele and provides an in vivo marker for *Drosophila* chromosome behavior. DNA Cell Biol. *18*, 457–462.

30. Fogarty, P., Kalpin, R.F., and Sullivan, W. (1994). The *Drosophila* maternal-effect mutation grapes causes a metaphase arrest at nuclear cycle 13. Development *120*, 2131–2142.

31. Sibon, O.C., Stevenson, V.A., and Theurkauf, W.E. (1997). DNA-replication checkpoint control at the *Drosophila* midblastula transition. Nature *388*, 93–97.

32. Sonoda, E., Matsusaka, T., Morrison, C., Vagnarelli, P., Hoshi, O., Ushiki, T., Nojima, K., Fukagawa, T., Waizenegger, I.C., Peters, J.M., et al. (2001). Scc1/Rad21/Mcd1 is required for sister chromatid cohesion and kinetochore function in vertebrate cells. Dev. Cell *1*, 759–770.

33. Hoque, M.T., and Ishikawa, F. (2002). Cohesin defects lead to premature sister chromatid separation, kinetochore dysfunction, and spindle-assembly checkpoint activation. J. Biol. Chem. *277*, 42306–42314.

34. Nicklas, R.B. (1997). How cells get the right chromosomes. Science *275*, 632–637.

35. Waters, J.C., Chen, R.H., Murray, A.W., and Salmon, E.D. (1998). Localization of Mad2 to kinetochores depends on microtubule attachment, not tension. J. Cell Biol. *141*, 1181–1191.

36. Gregson, H.C., Schmiesing, J.A., Kim, J.-S., Kobayashi, T., Zhou, S., and Yokomori, K. (2001). A potential role for human cohesin in mitotic spindle aster assembly. J. Biol. Chem. *276*, 47575–47582.

37. Murata-Hori, M., and Wang, Y. (2002). The kinase activity of aurora B is required for kinetochore-microtubule interactions during mitosis. Curr. Biol. *12*, 894–899.

38. Adams, R.R., Wheatleya, S.P., Gouldsworthy, A.M., Kandels-Lewis, S.E., Carmena, M., Smythe, C., Gerloff, D.L., and Earnshaw, W.C. (2000). INCENP binds the Aurora-related kinase

AIRK2 and is required to target it to chromosomes, the central spindle and cleavage furrow. Curr. Biol. *10*, 1075–1078.

39. Kaitna, S., Mendoza, M., Jantsch-Plunger, V., and Glotzer, M. (2000). Incenp and an aurora-like kinase form a complex essential for chromosome segregation and efficient completion of cytokinesis. Curr. Biol. *10*, 1172–1181.

40. Martineau-Thuillier, S., Andreassen, P.R., and Margolis, R.L. (1998). Colocalization of TD-60 and INCENP throughout G2 and mitosis: evidence for their possible interaction in signalling cytokinesis. Chromosoma *107*, 461–470.

41. Uren, A.G., Wong, L., Pakusch, M., Fowler, K.J., Burrows, F.J., Vaux, D.L., and Choo, K.H. (2000). Survivin and the inner centromere protein INCENP show similar cell-cycle localization and gene knockout phenotype. Curr. Biol. *10*, 1319–1328.

42. Wheatley, S.P., Carvalho, A., Vagnarelli, P., and Earnshaw, W.C. (2001). INCENP is required for proper targeting of Survivin to the centromeres and the anaphase spindle during mitosis. Curr. Biol. *11*, 886–890.

43. Birkenbihl, R., and Subramani, S. (1992). Cloning and characterization of rad21 an essential gene of *Schizosaccharomyces pombe* involved in DNA double-strand-break repair. Nucleic Acids Res. *20*, 6605–6611.